

**Minnesota Local Road Research Board (LRRB)
Investigation 864 and, MPR Project No. 6-(022)**

Recycled Asphalt Pavement:

MnROAD Study of Fractionated RAP

Task 4 Summary Report:

***Laboratory Testing of Conventional and Fractionated RAP
Bituminous Mixtures from MnROAD Phase 2 Construction***

Submitted to the LRRB and FHWA technical advisory panels:
May 29, 2012

Revised and submitted for approval June 14, 2012

Eddie N. Johnson and Timothy R. Clyne
*MnDOT Office of Materials and Road Research
1400 Gervais Avenue, Maplewood, Minnesota 55109*

Table of Contents

Chapter 1: Introduction	3
Acknowledgements	3
Background and Objectives	3
Chapter 2: Laboratory Testing Methods.....	5
Method 1 Dynamic Shear and Bending Beam Rheometer	5
Method 2 Direct Tension Test.....	6
Method 3 Double-Edge Notched Tension Test.....	6
Method 4 Indirect Tension Test	7
Method 5 Semi-Circular Bend Test	7
Method 6 Dynamic Modulus.....	7
Chapter 3: Test Results	9
Method 1 Dynamic Shear and Bending Beam Rheometer	9
Method 2 Direct Tension Test.....	10
Method 3 Double-Edge Notched Tension Test.....	13
Method 4 Indirect Tension Test	15
Mixture Creep Compliance	16
Method 5 Semi-Circular Bend	19
Method 6 Dynamic Modulus.....	23
Chapter 4: Activation and Blending of Recycled Asphalt	24
Materials.....	24
Methodology	24
Dynamic Modulus Testing	24
Binder Complex Modulus Testing	25
Hirsch Model.....	27
Discussion	30
Chapter 5: Conclusions and Observations	32
Summary and Recommendations.....	32
Conclusions	32
References	34

List of Figures

Figure 1 MnROAD layout.	4
Figure 2 DSR (L), and specimen between load plates (R).	5
Figure 3 BBR and specimen in load frame.	6
Figure 4 Specimen configuration for DENT test (7).	6
Figure 5 Detail of IDT (8).	7
Figure 6 Dynamic modulus specimen in testing chamber.	8
Figure 7 Ultimate Tensile Failure Stress of MnROAD's Phase II asphalt binders.	11
Figure 8 Tensile Strain at Failure of MnROAD's Phase II asphalt binders.	12
Figure 9 Tensile Strain at Failure of MnROAD's Phase I asphalt binders.	12
Figure 10 DENT Ultimate Tensile Failure Stress of MnROAD's Phase II asphalt binders.	13
Figure 11 DENT Tensile Strain at Failure of MnROAD's Phase II asphalt binders.	14
Figure 12 DENT Toughness of MnROAD's Phase II asphalt binders.	14
Figure 13 MnROAD Phase II IDT tension.	16
Figure 14 IDT Creep Results, (PG +10) -12.	17
Figure 15 IDT Creep Results, (PG +10).	18
Figure 16 IDT Creep Results, (PG +10) +12.	19
Figure 17 Fracture energy by mixture.	20
Figure 18 Fracture toughness by mixture.	20
Figure 19 Fracture energy versus temperature condition.	21
Figure 20 Fracture toughness versus temperature condition.	21
Figure 21 Fracture energy of MnROAD Phase II 0, 20, and 30% RAP.	22
Figure 22 Fracture toughness of MnROAD Phase II 0, 20, and 30% RAP.	23
Figure 23 Mixture dynamic modulus master curves.	25
Figure 24 Extracted asphalt binder master curves.	26
Figure 25 Example of shift factor vs. temperature curve for Cell 16.	28
Figure 26 Hirsch model results for PG 58-34 WMA RAP 20%, Cell 16.	29
Figure 27 Hirsch model results for PG 28-28 HMA RAP 20%, Cell 20.	29
Figure 28 Hirsch model results for PG 58-28 HMA FRAP 30%, Cell 21.	30
Figure 29 Hirsch model results for PG 58-34 HMA FRAP 30%, Cell 22.	30

List of Tables

Table 1 MnROAD Phase I Materials.	3
Table 2 MnROAD Phase II Bituminous Cell Boundaries.	4
Table 3 DSR Results for Asphalt Binders.	9
Table 4 BBR Results for Asphalt Binders.	9
Table 5 High PG Grade from Construction Samples.	10
Table 6 DT Binder Test Results for Materials Used During MnROAD Phase II (2008).	10
Table 7 DT Binder Test Results for Materials Used During MnROAD Phase I (1999).	11
Table 8 Phase II Mixtures Evaluated with IDT.	15
Table 9 IDT Tensile Strength Statistics, AASHTO T322.	16
Table 10 Predicted Fracture (Gf) Performance.	23
Table 11 Asphalt Mixture Types Included in Study.	24

Chapter 1: Introduction

Acknowledgements

The authors would like to thank technical staff at the Federal Highway Administration for mixture dynamic modulus testing. We also thank the staff at the MnDOT Chemical Laboratory for performing the asphalt binder testing, and Dr. Adam Zofka for his insights and discussions regarding data analysis. Finally, our appreciation is extended to the Local Road Research Board, Federal Highway Administration, and MnDOT for their financial support of this project.

Background and Objectives

This report represents task 4 of Local Road Research Board (LRRB) project number 864, Minnesota State Planning and Research project number MPR 06-(022) study entitled, “Recycled Asphalt Pavement: MnROAD Study of Fractionated RAP”. This report will summarize the laboratory testing performed on bituminous mixtures that were part of the MnROAD Phase II Construction (1). This report will present findings from laboratory testing and show how the test results will be compared with field performance.

Construction of the test sections was part of state project 8680-157, Additional details can be found in the MnROAD Phase II construction report (2) and other Investigation 864 task reports (3, 4, 5, and 6). Three fractionated RAP (FRAP) test cells and eight RAP test cells were constructed during Phase II. The source of all RAP material was the original MnROAD Phase I surface that was constructed in 1993 (3). Table 1 shows the locations of the MnROAD Phase I materials that were used for constructing RAP and FRAP cells during Phase II. Four different mixtures were developed for Phase I, utilizing two binder types, the same aggregates, and contained no recycled material. Phase I mixture were designed at 5.9 to 6.4% asphalt binder.

Table 1 MnROAD Phase I Materials

Cell No.	Penetration Grade	Viscosity Grade	PG Grade	% RAP
14, 20 – 23	120/150		58-28	0
16 – 19		AC-20	64-22	0

The FRAP experiment contained Cells 20, 21, and 22. The remaining RAP construction contained Cells 4, 15, 16, 17, 18, 19, 23, and 24. Boundaries, descriptions, and layout for the respective test cells are shown in Table 2 (2) and Figure 1.

Table 2 and Figure 1 show the relative location of the RAP/FRAP study cells (highlighted in red) on MnROAD’s Mainline (ML) and Low Volume Road (LVR). The binder Performance Grade (PG) included 64-34, 58-34, or 58-28. The thicknesses, in inches, of the pavements are denoted as follows: total thickness (non-wear course thickness + wear course thickness).

Several specialty mixtures, including PG’s 64-22, 64-34 and 70-28, were also constructed during Phase II as part of research unrelated to RAP performance. Selected test results from the specialty mixtures will be included in this report for comparison purposes.

Table 2 MnROAD Phase II Bituminous Cell Boundaries

Cell No.	HMA Mix Type: 12.5mm Dense Graded SuperPave	PG Binder Grade	% RAP	Structure (in) Wear + Nonwear
4	HMA	64-34	0	3
15	WMA	58-34	20	3
16 – 19	WMA	58-34	20	5 (2 + 3)
20	HMA	58-28	30	5 (2 + 3)
21	HMA + FRAP	58-28	30*	5 (2 + 3)
22	HMA + FRAP	58-34	30*	5 (2 + 3)
23	WMA	58-34	20	5 (2 + 3)
24	HMA	58-34	20	3

*Denotes that RAP was split on 1/4-in. screen

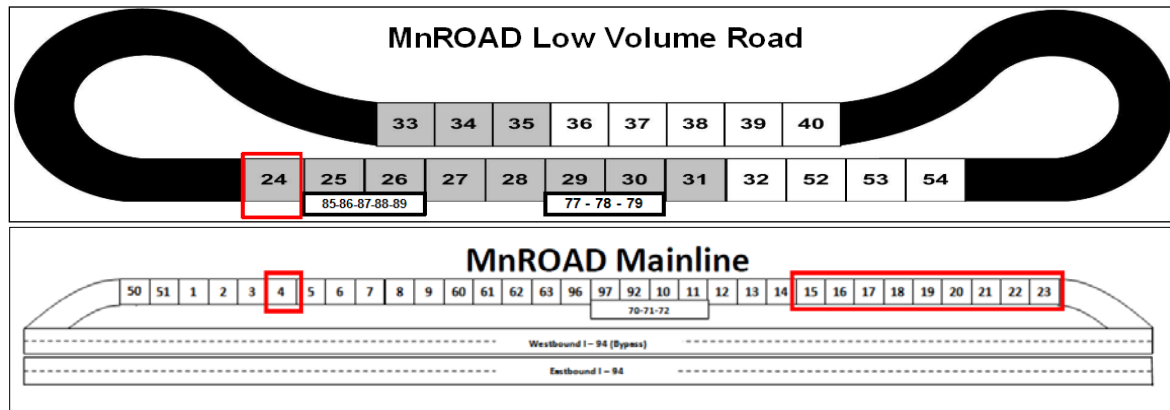


Figure 1 MnROAD layout.

The asphalt, aggregate base, subbase, and granular fill layers were of identical thickness in Cells 19 through 23. In the region that included Cells 15 – 19 and 23 (warm mix) the asphalt mat was paved in a continuous process. Cell 24’s mixture used the same construction materials, except it was produced at hot mix temperatures. Cells 20 and 21 were constructed using PG 58-28 asphalt binder. PG 58-34 asphalt was used in all of the remaining cells except for Cell 4, where the grade changed to PG 64-34, used no RAP, and was produced as hot mix. Base material types vary within this part of MnROAD. See reference (2) for additional construction details.

Chapter 2: Laboratory Testing Methods

MnROAD Phase II mixtures and binders were evaluated with a variety of laboratory tests. Tension and rheometer tests were used to evaluate the binders. Mixtures were evaluated with fracture and modulus tests. Short descriptions of the methods are provided in this chapter.

Method 1 Dynamic Shear and Bending Beam Rheometer

Dynamic Shear Rheometer (DSR) is an asphalt binder test that yields data used to evaluate the high-temperature performance grade of asphalt binders and develop the master curve of modulus (G^*) versus frequency. The master curves provide information on the relative stiffness of asphalts for a given loading rate or temperature. G^* performance at low frequencies are related to performance at high temperatures. The same is true for high frequencies and low temperatures. Results are reported in terms of stress (kPa). Figure 2 and shows a DSR with an asphalt binder specimen.



Figure 2 DSR (L), and specimen between load plates (R).

The Bending Beam Rheometer (BBR) is an asphalt binder test that yields data for evaluating the low-temperature performance grade of asphalt binder. Prismatic beams of asphalt binder are evaluated in 3-point bending at low temperature. Figure 3 shows a BBR load frame applying force. Results are reported in terms of stiffness and also the slope of the BBR curve (m-value).

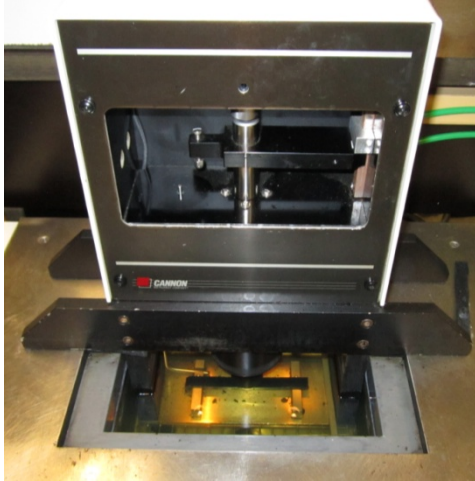


Figure 3 BBR and specimen in load frame.

Method 2 Direct Tension Test

Direct Tension Test (DT) is an asphalt binder test method that yields parameters useful in evaluating the thermal cracking performance of asphalt mixtures. Dog-bone shaped asphalt specimens are subjected to tension. Results are reported in terms of stress and critical cracking temperature.

Method 3 Double-Edge Notched Tension Test

The Double-Edge Notched Tension Test (DENT) is performed on asphalt binders, and yields parameters useful in evaluating the thermal cracking and fatigue performance of asphalt mixtures. Notches are formed on both sides of a dog-bone shaped asphalt specimen, direct tension is applied, and the stress intensity factor is reported. Zofka and Marasteanu (2007) compared DENT and DT for a number of different asphalts. They found DENT useful for estimating critical temperature, and more repeatable than DT (7).

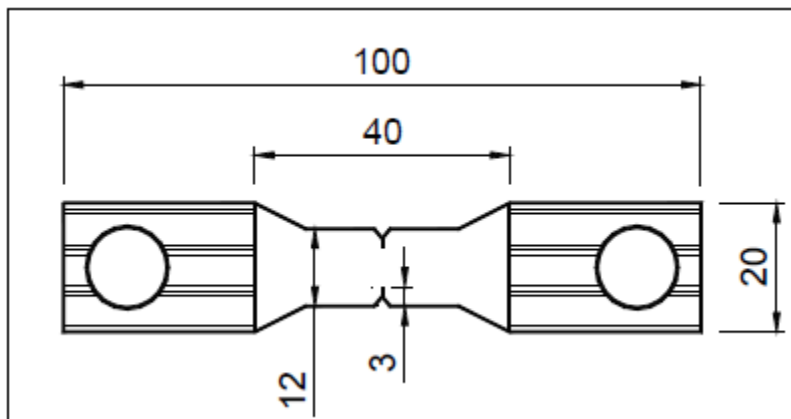


Figure 4 Specimen configuration for DENT test (7).

Method 4 Indirect Tension Test

The Indirect Tension Test (IDT) is performed on asphalt mixtures, and can yield parameters useful in evaluating the strength of asphalt mixtures. Cylindrical specimens having a diameter to thickness ratio of 3:1 are produced from laboratory-produced cylinders or field cores. The specimens are tested by applying load across the diameter of the cylinder (Figure 5). Test results are reported in terms of tensile strength or creep compliance.



Figure 5 Detail of IDT (8).

Method 5 Semi-Circular Bend Test

The Semi-Circular Bend Test (SCB) is performed on asphalt mixtures, and yields fracture properties useful in evaluating the thermal cracking performance of asphalt mixtures. SCB specimen production is similar to IDT, but includes subdividing the cylinder with a cut that effectively produces specimen having: one curved edge, one flat edge, and two “D” shaped faces. Each specimen is oriented with the curved edge up and then tested in a 3-point flexural configuration. Crack initiation is promoted and controlled by a notch cut into midpoint of the flat edge.

Method 6 Dynamic Modulus

Dynamic Modulus ($|E^*|$) testing is performed on asphalt mixtures, and yields data used to develop master curves of $|E^*|$ versus frequency. Data is reported in terms of stiffness, frequency, and temperature. Master curves likewise provide information on the relative stiffness of asphalt mixtures for a given loading rate or temperature. $|E^*|$ performance at low frequencies are related to performance at high temperatures. The same is true for high frequencies and low temperatures. E^* specimens are produced from either laboratory-compacted pucks of asphalt mixture or from

field cores. Typical diameter to height ratio is 2:3. Figure 6 shows a laboratory-produced E* specimen in a test chamber.



Figure 6 Dynamic modulus specimen in testing chamber.

Chapter 3: Test Results

Binder and mixture testing was performed by the University of Minnesota Department of Civil Engineering and MnDOT's Office of Materials and Road Research. The values for following data tables and plots were obtained from the MnROAD database and laboratory reports.

Method 1 Dynamic Shear and Bending Beam Rheometer

Samples of asphalts were obtained from the plant for conditioning and verification of PG grading. Test results are shown in Table 3 and Table 4.

Table 3 DSR Results for Asphalt Binders

MnDOT ID	Sample ID	Study Cells	Test Temp, °C	Original binder G*/Sin δ, kPa	RTFO G*/Sin δ, kPa	PAV G*/Sin δ, kPa	PAV Phase angle
AC 746	58-28	20, 21	58	1.153	3.030	3579	51.10
AC 747	58-34	22	58	1.155	2.446	2475	49.03
AC 748	58-34 WMA	15-19, 23	58	1.557	4.763	2502	42.32
AC 749	64-22	NA	64	1.103	2.711	3370	52.30
AC 750	64-34	4	64	1.209	2.803	2016	50.78
AC 751	70-28	NA	70	1.192	2.726	1342	51.68

Table 4 BBR Results for Asphalt Binders

MnDOT ID	Study Cells	BBR Test Temp °C	BBR Stiffness, MPa	BBR Mvalue	BBR Test Temp °C	BBR Stiffness, MPa	BBR Mvalue	Low Temp Grade, °C
AC 746	20, 21	-18	218	0.338	-24	440	0.283	-31.3
AC 747	22	-24	217	0.339	-30	363	0.264	-37.1
AC 748	15-19, 23	-24	208	0.330	-30	365	0.275	-37.3
AC 749	NA	-12	173	0.343	-18	296	0.292	-24.0
AC 750	4	-24	165	0.349	-30	418	0.283	-38.5
AC 751	NA	-18	147	0.360	-24	369	0.279	-32.4

Bituminous samples, in the form of either loose mix construction samples or pavement cores, were obtained from MnROAD. Asphalt binder was extracted and recovered from the samples and then evaluated for high temperature PG grade. The results are in Table 5. Note that the extracted asphalt content from the recycled materials closely resembles the binder content of Phase I mixtures that were described earlier.

Verification BBR and DSR test results showed that the plant AC samples and blended BC asphalt mixtures properties were adequate for the intended designs. Blended BC tests satisfied PG requirements by an excess of 2.6 to 10.1 degrees and AC tests exceeded by 2 to 4.5 degrees.

Table 5 High PG Grade from Construction Samples

MnDOT ID	Sample	AC %	DSR PG Grade
BC09-0014	WMA Wear 58-34	5.04	68.1
BC09-0015	WMA Non-Wear 58-34	5.60	67.9
BC08-0116	30% RAP 58-28 Wear	5.32	64.7
BC08-0117	30% RAP 58-28 Non-Wear	5.58	64.2
BC08-0118	30% FRAP 58-28 Wear	5.25	64.9
BC08-0119	30% FRAP 58-28 Non-Wear	5.51	63.6
BC08-0120	30% FRAP 58-34 Wear	5.49	61.5
BC08-0121	30% FRAP 58-34 Non-Wear	5.64	62.9
BC08-0123	WMA Control 58-34	5.45	60.6
BC08-0124	Crushed millings	6.01	69.0
BC08-0125	Fine RAP	6.76	71.2
BC08-0126	Coarse RAP	4.89	69.9
BC08-0124	Crushed millings	5.9	Not tested
BC08-0125	Fine RAP	6.4	Not tested
BC08-0126	Coarse RAP	5.2	Not tested

Method 2 Direct Tension Test

Direct Tension Testing was performed on binders extracted from the fine-fraction, coarse-fraction, and standard combined-fractions of MnROAD RAP. Testing was also performed on a variety of PG-graded binder samples conditioned using the RTFO-PAV procedures. The strain application rate was 3% per minute. Refer to Marasteanu et al. (9) for additional testing details.

As shown in Table 6, ultimate failure stress ranged from 1.34 to 6.26 MPa for the overall data set. The overall coefficient of variation (CV) was 21.5%. Ultimate failure strain ranged from 0.12 to 4.0% with an overall CV of 73.2%. This level of variation is anticipated due to the nature of the test procedure.

Table 6 DT Binder Test Results for Materials Used During MnROAD Phase II (2008)

	Strain, %	Stress, MPa
<i>N</i>	92	92
Mean	1.1963	4.2113
SD	0.8756	0.9066
Min	0.1200	1.3400
1st Q	0.5925	3.6625
Median	0.9050	4.2400
3rd Q	1.4500	4.8350
Max	4.0000	6.2600

As a comparison, Table 7 presents DT statistics for materials used during the MnROAD Phase I construction in 1999.

Table 7 DT Binder Test Results for Materials Used During MnROAD Phase I (1999)

	Strain, %	Stress, MPa
N	24	24
Mean	1.4621	3.2713
SD	1.6326	0.7753
Min	0.1400	1.8600
1st Q	0.2650	2.8400
Median	0.7550	3.1050
3rd Q	2.6175	3.6400
Max	6.5200	5.7000

A smaller statistical sampling was available from the 1999 data. Phase I material showed a larger DT standard deviation despite the fact that none of the 1999 binders contained recycled asphalt. DT results are charted as box-and-whiskers plots from Figure 7 to Figure 9.

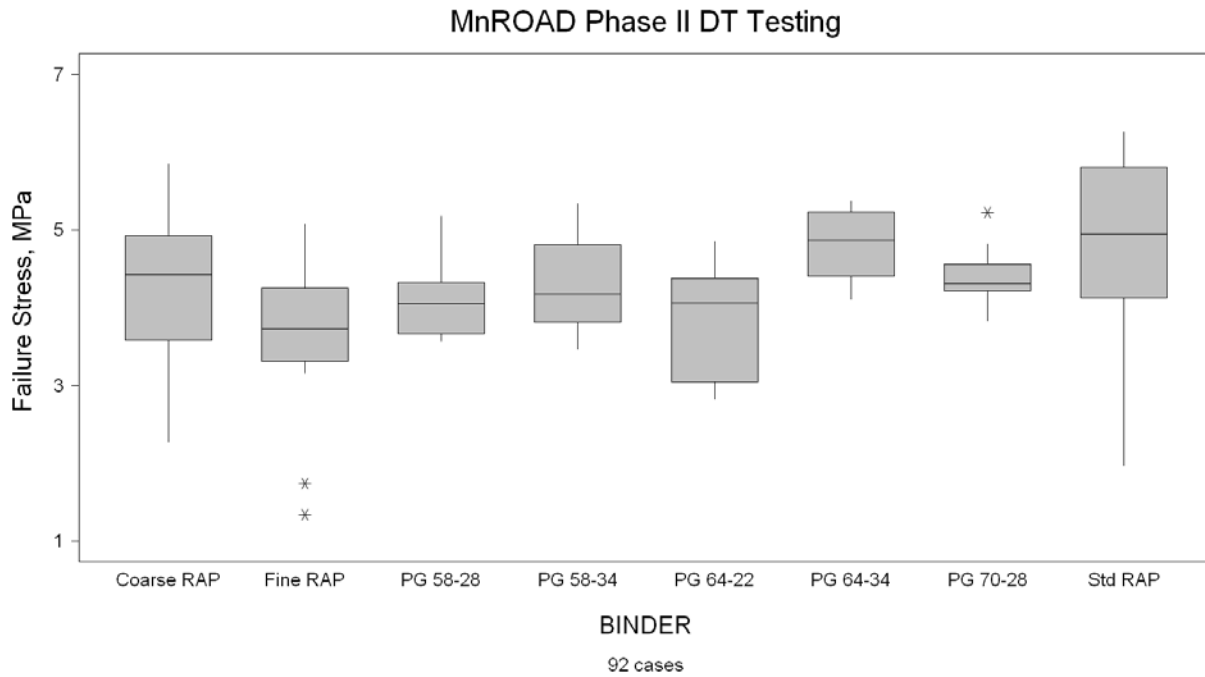


Figure 7 Ultimate Tensile Failure Stress of MnROAD’s Phase II asphalt binders.

All binders were quite similar in ultimate tensile failure stress. Approximately 87% of the Phase II failure stress data fell between 2.8 and 5.4 MPa.

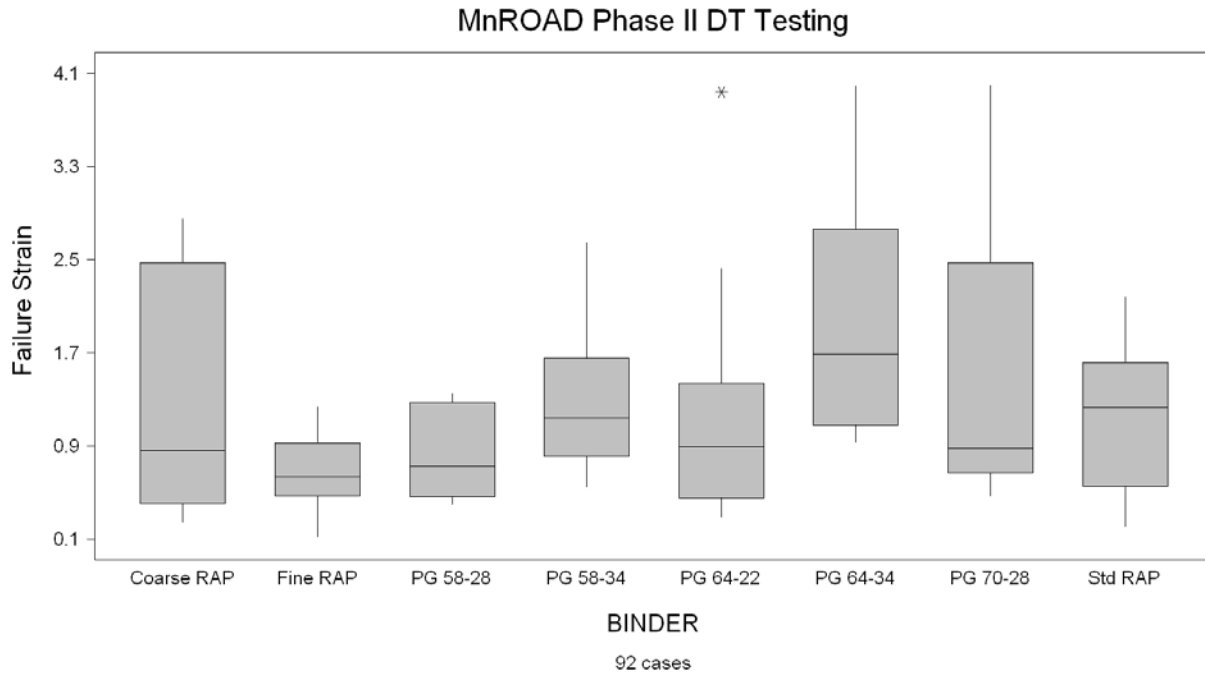


Figure 8 Tensile Strain at Failure of MnROAD’s Phase II asphalt binders.

Tensile failure strain showed some differentiation between Phase II binder materials, where tensile strain data followed a skewed frequency distribution and approximately 77% of the data was distributed below strain values of 1.5%.

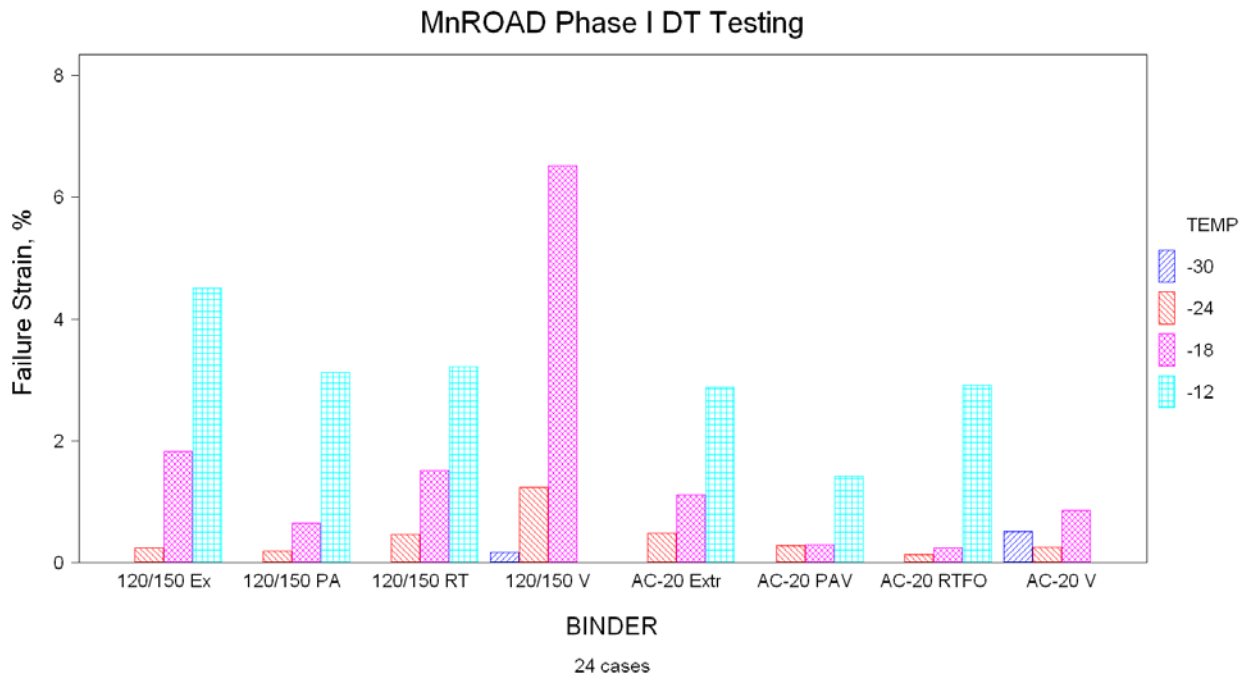


Figure 9 Tensile Strain at Failure of MnROAD’s Phase I asphalt binders.

Method 3 Double-Edge Notched Tension Test

Double-Edge Notched Tension was performed on PAV residue from AC samples obtained from the plant. RAP was also included in the testing. Standard, coarse, and fine RAP fractions were extracted and then tested without PAV treatment. Most of the asphalt materials performed within a range below 1.0 MPa. However, the PG 64-34 and 70-28 binders developed notably more stress, with data generally falling between 0.8 and 1.5 MPa. The two binders also developed notably greater strain levels and toughness compared with the rest of the materials.

Differences were also apparent between the hot-mix and warm-mix versions of the PG 58-34 binders, where the PG 58-34 (hot) was measured to have somewhat higher median levels of stress, strain, and toughness. DENT results are presented in Figure 10 through Figure 12. Refer to Marasteanu et al. (9) for additional testing details.

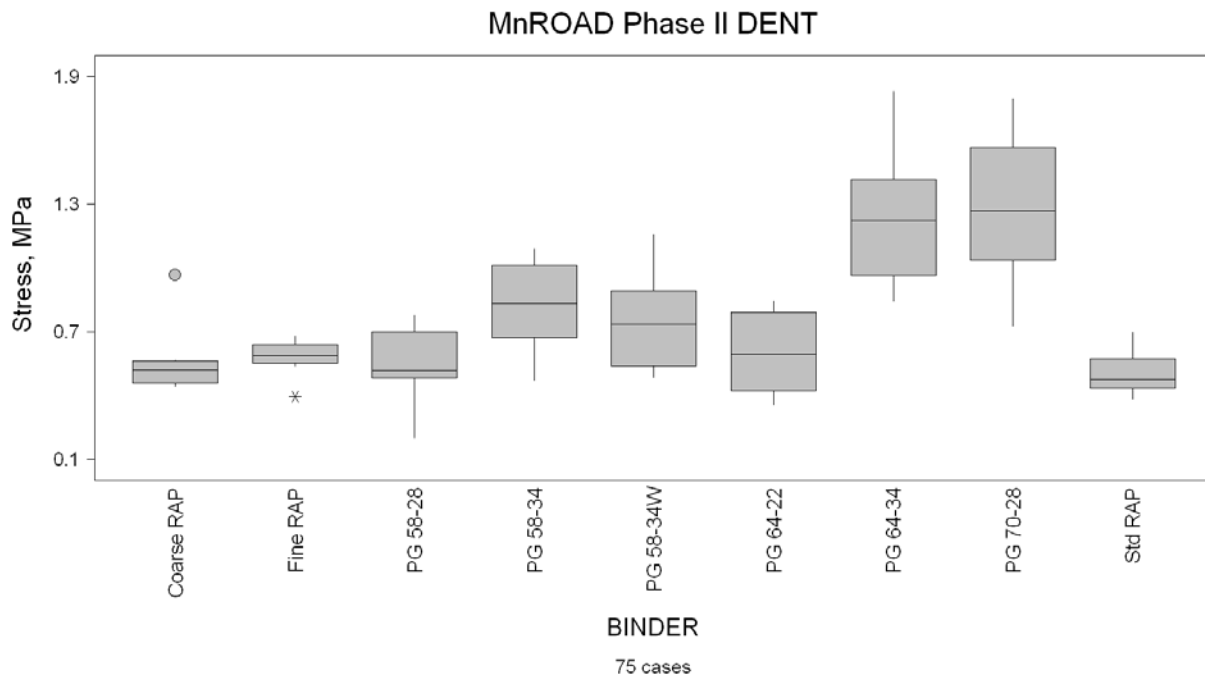


Figure 10 DENT Ultimate Tensile Failure Stress of MnROAD's Phase II asphalt binders.

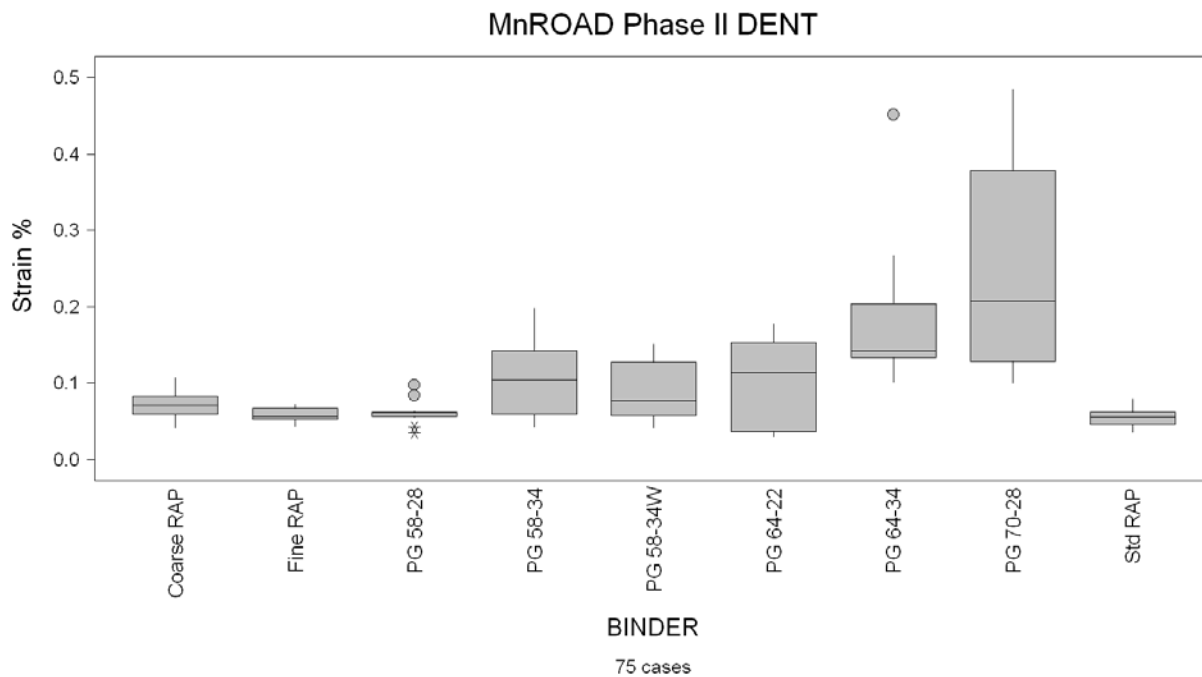


Figure 11 DENT Tensile Strain at Failure of MnROAD’s Phase II asphalt binders.

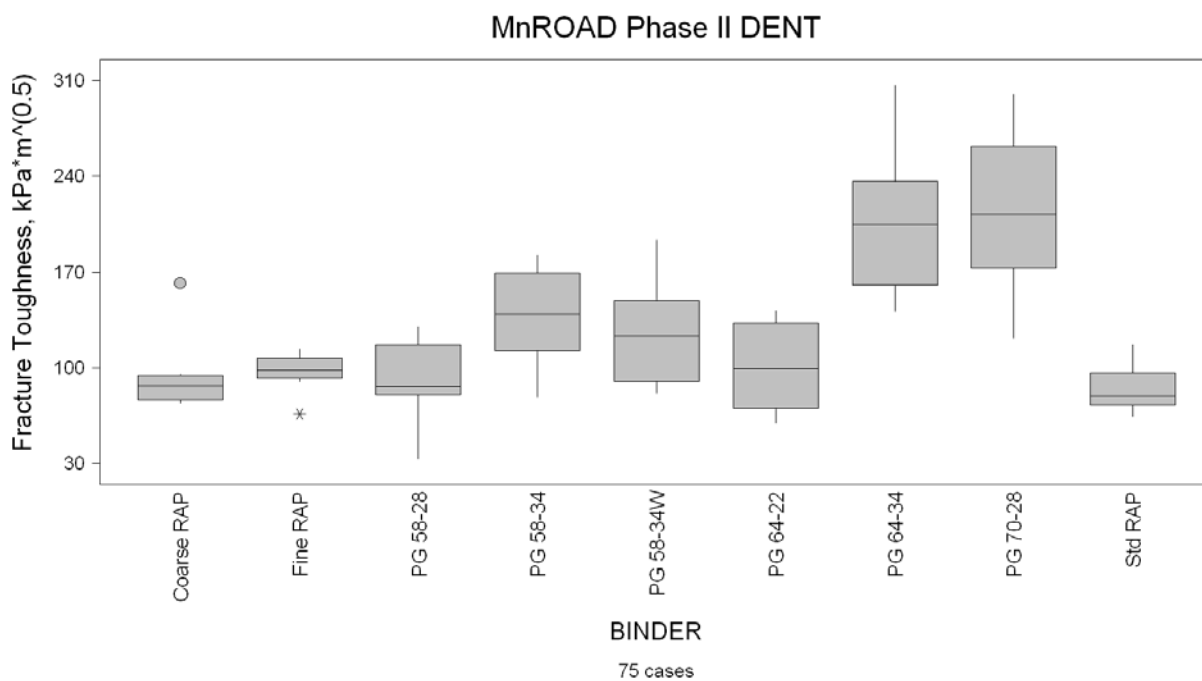


Figure 12 DENT Toughness of MnROAD’s Phase II asphalt binders.

Method 4 Indirect Tension Test

IDT test temperatures for nine traffic-lane mixtures are given in Table 8. Testing was performed at three temperatures (°C), later referred to as low, intermediate, and high. Refer to Marasteanu et al. (9) for additional testing details and comments on relaxation modulus.

- (PG low limit + 10) + 12
- (PG low limit + 10)
- (PG low limit + 10) - 12

Table 8 Phase II Mixtures Evaluated with IDT

Mix	Process	PG Binder Grade	% RAP	Test Temperature, °C
12.5mm Superpave described in Table 2	HMA	64-34	0	-36, -24, -12
	WMA	58-34	20	-36, -24, -12
	WMA	58-34	20	-36, -24, -12
	HMA	58-28	30	-30, -18, -6
	HMA + FRAP	58-28	30	-30, -18, -6
	HMA + FRAP	58-34	30	-36, -24, -12
	HMA	58-34	20	-36, -24, -12
Taconite Tailings	HMA	64-34	0	-36, -24, -12
Ultra Thin Bonded Wear	HMA – UT	64-34	0	-30, -18, -6
Porous Asphalt	HMA	70-28	0	-36, -24, -12

**Nonwear mixture

Tensile stress results are shown in Figure 13 and Table 9, where the first six entries show the relative performance of dense-graded 12.5-mm mixtures. The three remaining entries show IDT tensile performance of 4.75-mm, Ultra-Thin Bonded Wear, and porous bituminous mixtures.

The average IDT tensile strengths and range of values produced by mixtures within the group of six Fractionated/RAP/dense-graded mixtures were apparently similar when compared to results from the remaining mixtures.

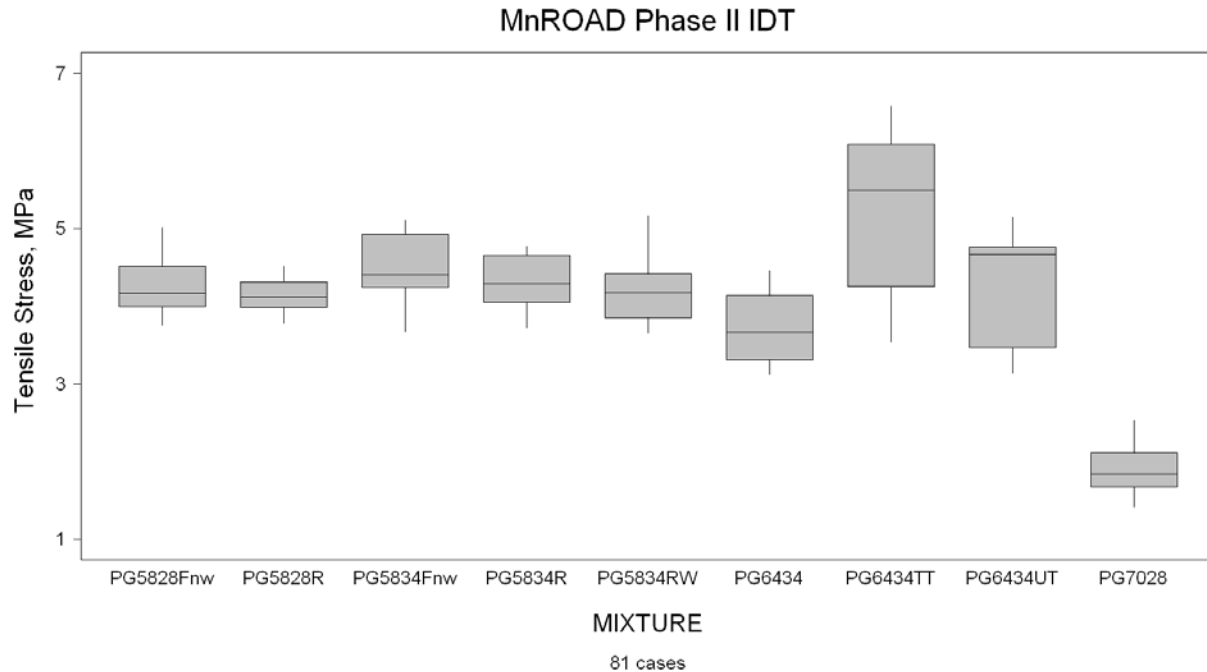


Figure 13 MnROAD Phase II IDT tension.

Table 9 IDT Tensile Strength Statistics, AASHTO T322

Mixture	Comment	Production	Recycle	RAP %	N	Mean, GPa	StDev
PG58-28Fnw	Nonwear	HMA	FRAP	30	9	4.2943	0.4695
PG58-28R	Wear	HMA	RAP	30	9	4.1484	0.2485
PG58-34Fnw	Nonwear	HMA	FRAP	30	9	4.483	0.4541
PG58-34R	Wear	HMA	RAP	20	9	4.3066	0.369
PG58-34RW	Wear	WMA	RAP	20	9	4.2474	0.5224
PG64-34	Wear	HMA		0	9	3.6806	0.5005
PG64-34TT	Wear	4.75 HMA		0	9	5.1653	1.1274
PG64-34UT	Wear	UT HMA		0	9	4.2563	0.7799
PG70-28	Wear	Porous HMA		0	9	1.8922	0.3469

Mixture Creep Compliance

The creep compliance of each mixture was generated using AASHTO T322. Results are presented below.

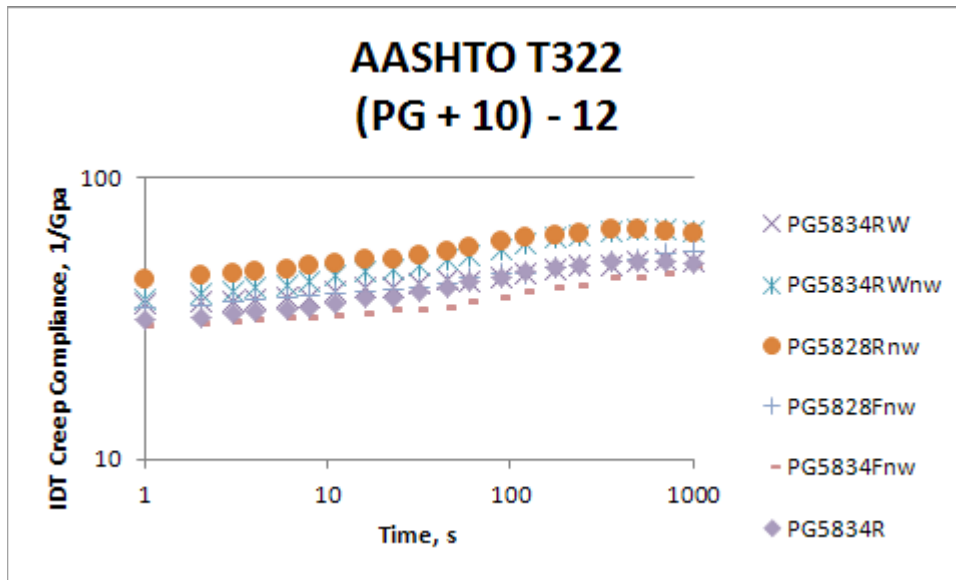


Figure 14 IDT Creep Results, (PG +10) -12.

At (PG + 10) -12 conditions the set of PG58-34 mixtures performed such that compliance values were ordered greatest to least:

- WMA-20% RAP-nonwear
- Between 1 and 100 seconds WMA-20% RAP generated values greater than HMA-30% RAP. After 100 seconds they were nearly equivalent.
- HMA-30% FRAP-nonwear

Also at (PG + 10) -12 conditions, the set of PG58-28 mixtures performed such that compliance values were ordered greatest to least:

- 20% RAP-nonwear generated the greatest values of all mixtures up to 178 seconds, when compliance values became approximately equivalent to PG58-34 WMA-20% RAP-nonwear.
- HMA-30% FRAP-nonwear. The IDT creep of this mix was approximately equivalent to PG 58-34 WMA-20% RAP.

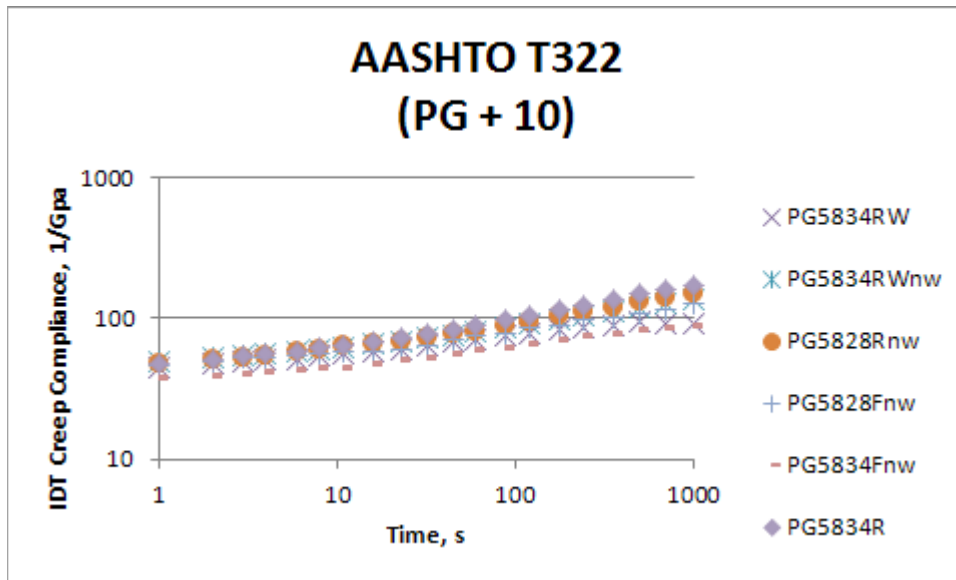


Figure 15 IDT Creep Results, (PG +10).

At (PG + 10) conditions the set of PG58-34 mixtures performed such that compliance values were ordered greatest to least:

- HMA-30% RAP and WMA-20% RAP-nonwear, and were nearly equivalent prior to 60 seconds. After 60 seconds the HMA-20% RAP mixture generated the greatest values relative to other PG58-34 mixtures.
- WMA-20% RAP
- HMA-30% FRAP

Also at (PG + 10) conditions, the set of PG58-28 mixtures performed such that compliance values were ordered greatest to least:

- 20% RAP-nonwear. Up to 60 seconds this mix was equivalent, and afterward less than, PG58-34 HMA-30% RAP.
- HMA-30% FRAP-nonwear. This mix was approximately equivalent to WMA-20% RAP.

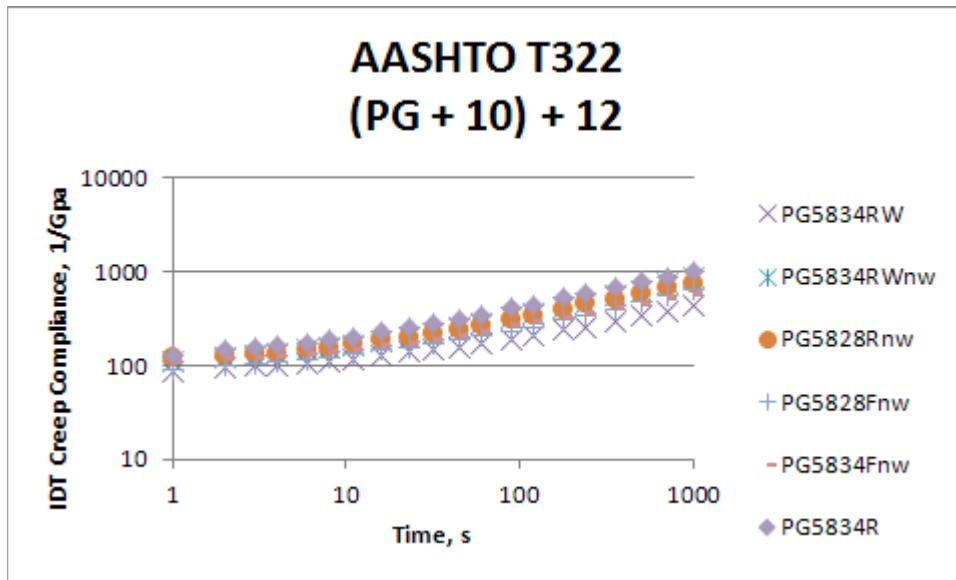


Figure 16 IDT Creep Results, (PG +10) +12.

At (PG + 10) +12 conditions the set of PG58-34 mixtures performed such that compliance values were ordered greatest to least:

- HMA-30% RAP
- WMA-20% RAP-nonwear
- HMA-30% FRAP
- WMA-20% RAP

Also at (PG + 10) +12 conditions, the set of PG58-28 mixtures performed such that compliance values were ordered greatest to least:

- 20% RAP-nonwear. This mix was approximately equivalent to PG58-34 WMA-20% RAP-nonwear.
- HMA-30% FRAP-nonwear. This mix was approximately equivalent to HMA-30% FRAP-nonwear.

Method 5 Semi-Circular Bend

Semi-Circular Bend testing was performed on mixture specimens. Toughness (K_{IC}) and fracture energy (G_f) were calculated from testing performed at three temperatures ($^{\circ}C$).

- (PG +10) - 12
- (PG +10)
- (PG +10) + 12

Fracture energy was calculated according to RILEM TC 50-FMC. Aggregate results for the Phase II mixtures are shown from Figure 17 to Figure 20. Refer to Marasteanu et al. (9) for additional testing details.

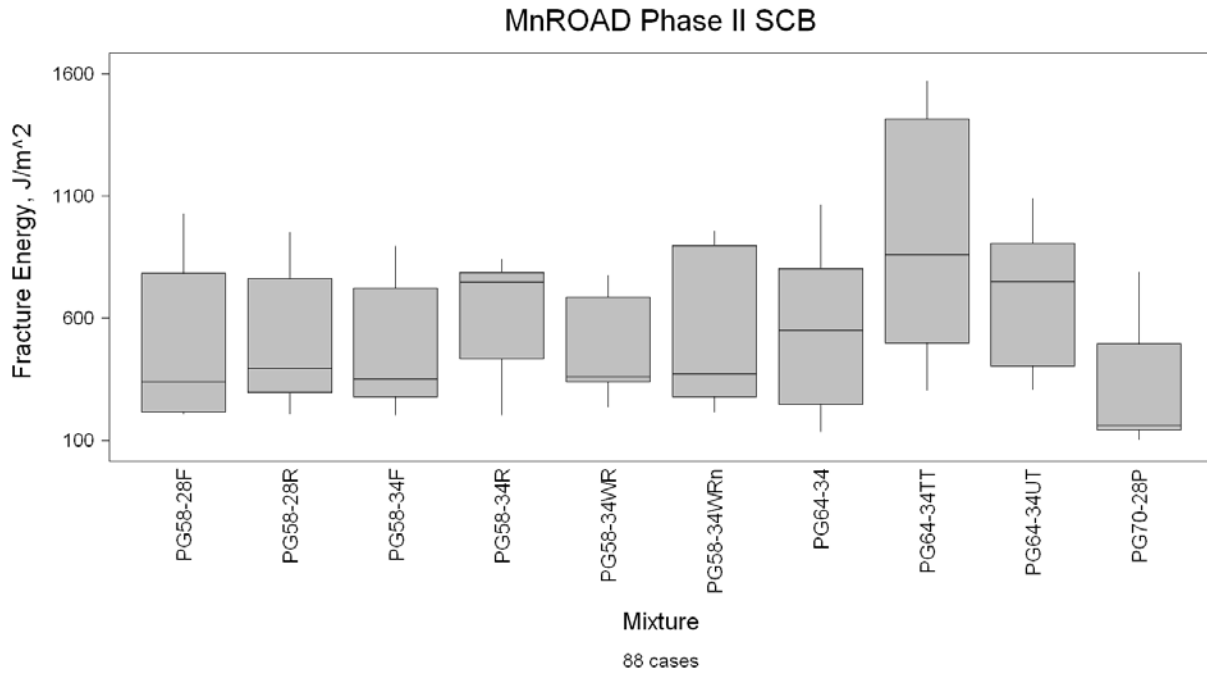


Figure 17 Fracture energy by mixture.

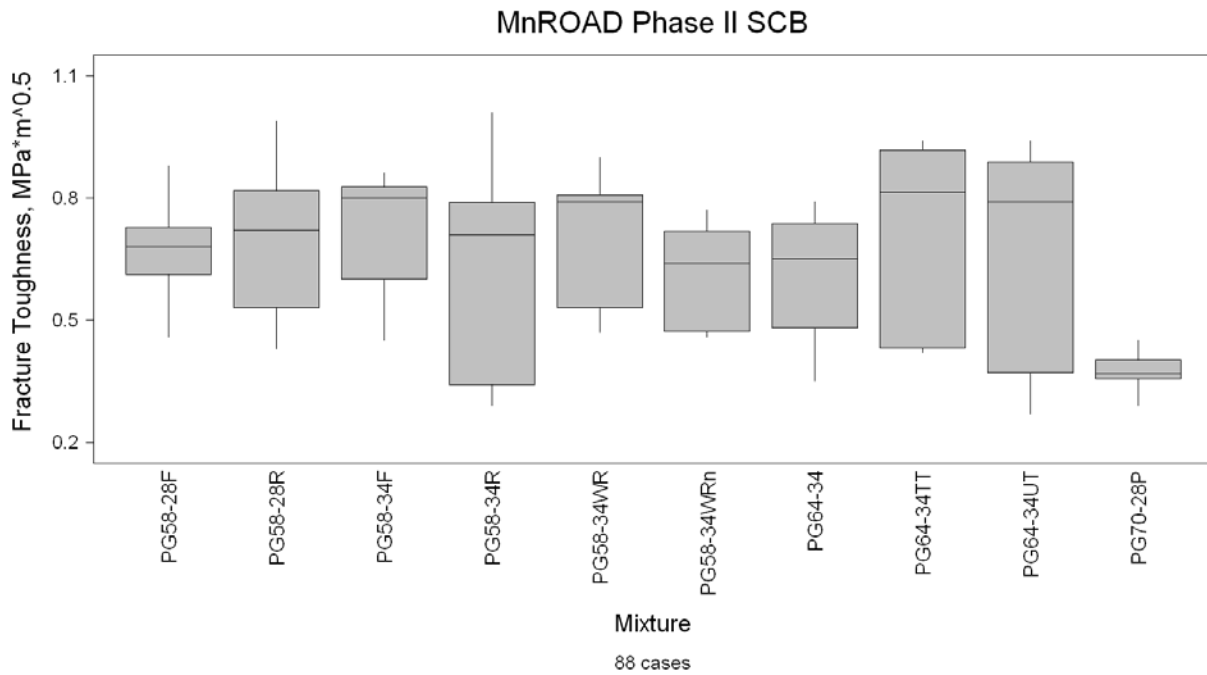


Figure 18 Fracture toughness by mixture.

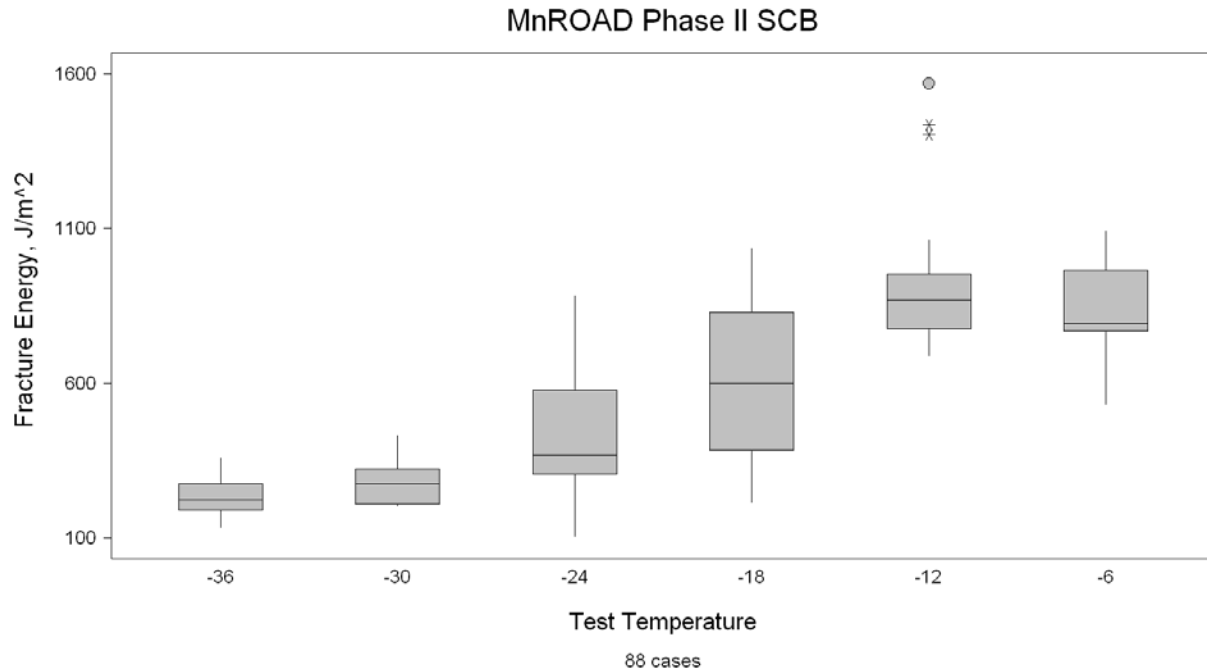


Figure 19 Fracture energy versus temperature condition.

Fracture toughness was also calculated from SCB test results. A plot of toughness grouped by test temperature is shown in Figure 20.

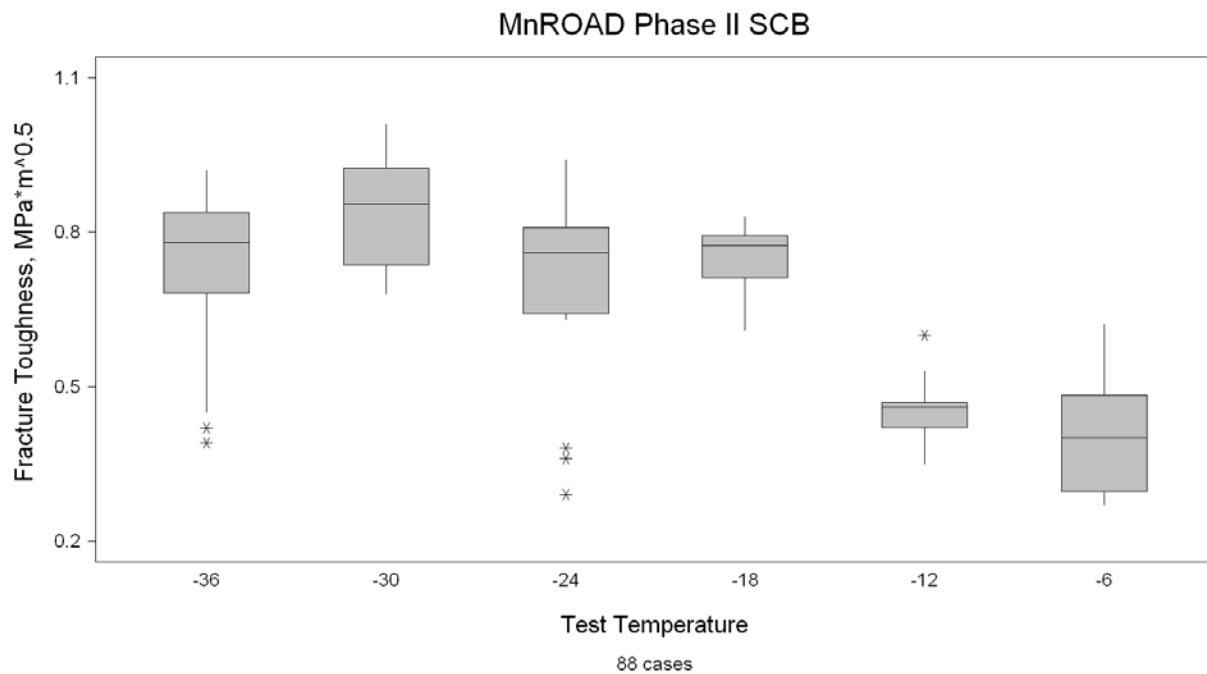


Figure 20 Fracture toughness versus temperature condition.

A plot of fracture energy grouped by recycled asphalt percentage is shown in Figure 21. The figure also shows best-fit exponential curves along with their equation and R-square value. A similar treatment for toughness is plotted in Figure 22, including linear trend lines. Several trends can be identified from the figures. For fracture energy:

- Three distinct trends emerged for mixtures that were grouped by recycle percentage.

For toughness:

- 0% recycled group overlapped with the 20% and 30% groups near the test temperature extremes.
- 0% and 30% performance equalized at approximately -30 °C.
- 20% recycle group (composed of PG58-34 WMA and HMA mixtures) maintained relatively lower toughness values through the low temperature performance range.

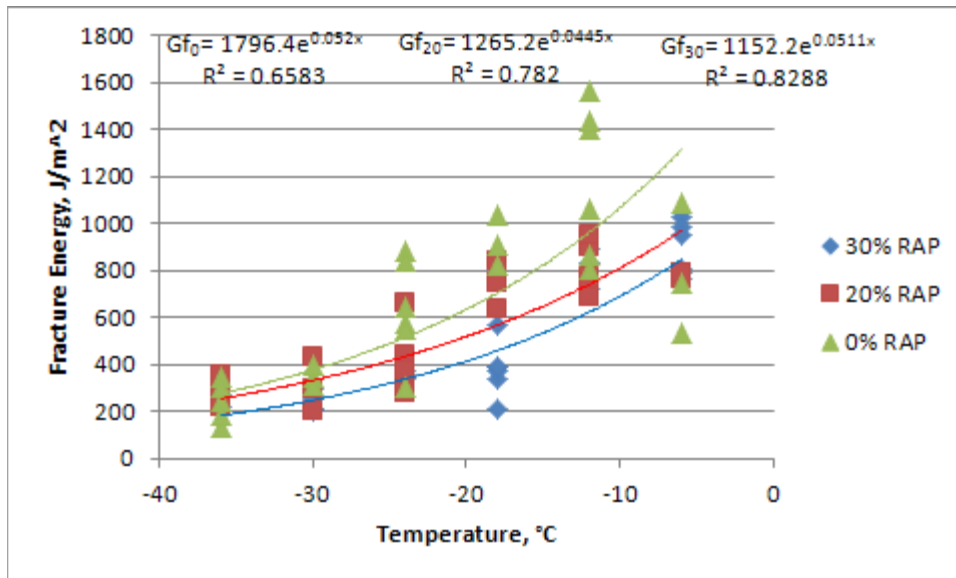


Figure 21 Fracture energy of MnROAD Phase II 0, 20, and 30% RAP.

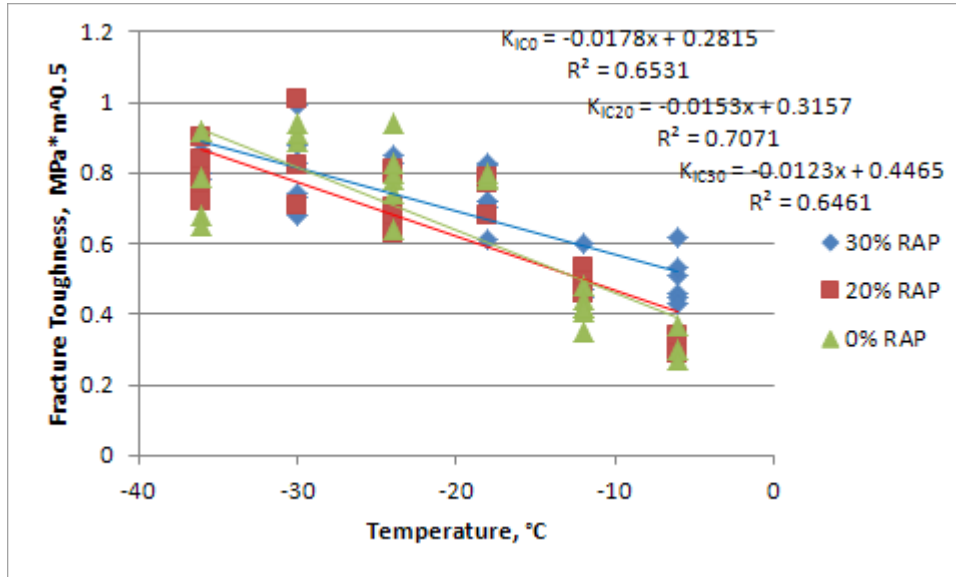


Figure 22 Fracture toughness of MnROAD Phase II 0, 20, and 30% RAP.

Table 10 presents fracture energy as functions of the best-fit equations from Figure 21. The equations were used to compare the temperatures where groups attained fracture energy performance levels of 350 to 400 J/m²; values where field performance would potentially be affected.

Table 10 Predicted Fracture (Gf) Performance

Temperature °C	Fracture Energy, J/m ²		
	0% RAP	20% RAP	30% RAP
-20.70	612	504	400
-23.32	534	448	350
-25.88	468	400	307
-28.88	400	350	263
-31.45	350	312	231
Fit	$1796.4e^{0.052x}$	$1265.2e^{0.0445x}$	$1152.2e^{0.0511x}$
R-squared	0.6583	0.782	0.8288

Method 6 Dynamic Modulus

Dynamic modulus testing will be discussed in greater detail in the chapter “Activation and Blending of Recycled Asphalt”.

The testing was performed by the Federal Highway Administration via their Mobile Asphalt Laboratory. The tests were run at four temperatures (4.4, 21.1, 37.8, and 54.4 °C) and six frequencies per temperature (25, 10, 5, 1, 0.5, and 0.1 Hz). Three replicate tests were performed on each mixture. Dynamic modulus data on Cell 24, the control section for warm mix asphalt, is not yet available.

Chapter 4: Activation and Blending of Recycled Asphalt

Several mixtures from the MnROAD RAP study were analyzed in an attempt to identify binder activation, or intermingling of recycled asphalt with virgin asphalt, that may have occurred during plant mixing.

Materials

The pavement materials used for this study were collected from five MnROAD test cells: four on the MnROAD Mainline and one on the Low Volume Road. They were all Level 4 Superpave mixtures (3-10 million ESALs) composed of various binder grades and RAP levels. The same virgin aggregates (primarily granite) were used for all mixtures, and the RAP material originated from a single source, namely crushed millings from the original MnROAD test sections that were removed. See Table 11 for a description.

Table 11 Asphalt Mixture Types Included in Study

Cell	Mix Description	PG Grade	RAP
16	Warm mix (chemical additive)	58-34	20% standard
20	HMA	58-28	30% standard
21	HMA	58-28	30% fractionated
22	HMA	58-34	30% fractionated
24	Warm mix control	58-34	20% standard

The asphalt mixtures were sampled at the job site from the truck box immediately before paving. Some mixture was taken back to the laboratory, and the binder was extracted and recovered according to AASHTO T319 (10), with the exception to the standard of using toluene as the extraction agent.

Methodology

A combination of mixture and binder testing, along with the use of the Hirsch Model, was used to evaluate the activation of recycled asphalt binder.

Dynamic Modulus Testing

A master curve of dynamic modulus vs. frequency was created for each mixture using the sigmoidal function shown in Equation 1, which was developed as part of NCHRP Project 1-37A (11).

$$\log(E^*) = \delta + \frac{\alpha}{1 + e^{\beta + \gamma(\log \omega_r)}}$$

Equation 1

where

E^* = dynamic modulus

ω_r = reduced frequency

δ = minimum value of E^*

$\delta + \alpha =$ maximum value of E^*
 $\beta, \gamma =$ parameters describing the shape of the sigmoidal function

Each master curve was fit at a reference temperature of 54.4°C. The curve fit was performed using a simple least squares method in Excel, where the four parameters ($\alpha, \beta, \delta, \gamma$) were fit along with the shift factor for each test temperature. See Figure 23 for a plot of the master curves for each of the mixtures.

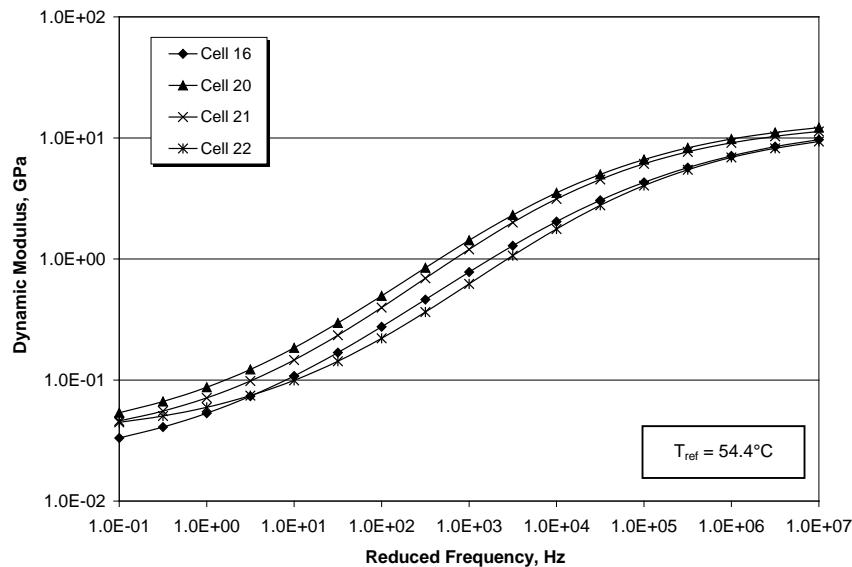


Figure 23 Mixture dynamic modulus master curves.

As expected, the two mixtures with PG 58-28 binder were stiffer than those with PG 58-34 binder. These two stiffer curves show very slight differences, indicating that fractionating the RAP piles can produce slightly softer (and therefore more resistant to cracking) mixtures. The mixture from Cell 22 was generally the softest across most of the temperature regime, indicating that a softer binder produced a softer mixture than those made with PG 58-28 binder. The warm mix was by far the softest material at high temperatures (or low frequencies shown on the left of the plot). This is likely due to the combination of the PG 58-34 binder, lower RAP content (20%) than the other mixtures (30%), and reduced binder aging due to the lower production temperatures that are associated with the warm mix technology.

Binder Complex Modulus Testing

The next step was to perform frequency sweep testing on the dynamic shear rheometer (DSR) on the binders that were extracted and recovered from the mixtures. The tests were run from 34°C to 76°C at 6° intervals on standard 25 mm parallel plates. At each temperature the frequency ranged from 1 to 100 rad/s.

The DSR data was then used to construct master curves for each binder using the CAM model (12) shown in Equation 2.

$$|G^*(\omega)| = G_g \left[1 + \left(\frac{\omega_c}{\omega} \right)^v \right]^{-\frac{w}{v}}$$

Equation 2

where

$|G^*(\omega)|$ = complex modulus as a function of frequency ω (GPa)
 G_g = glassy modulus (log [G_g] is considered fixed at 9.1)
 ω_c , v , w = model parameters

Each master curve was fit at a reference temperature of 58°C. The curves were fit using a non-linear least-squared regression technique built in to a commercially available statistics program called SigmaStat. Like the mixture master curves, this program fit the model parameters along with the shift factor at each temperature. See Figure 24 for plots of the extracted binder master curves.

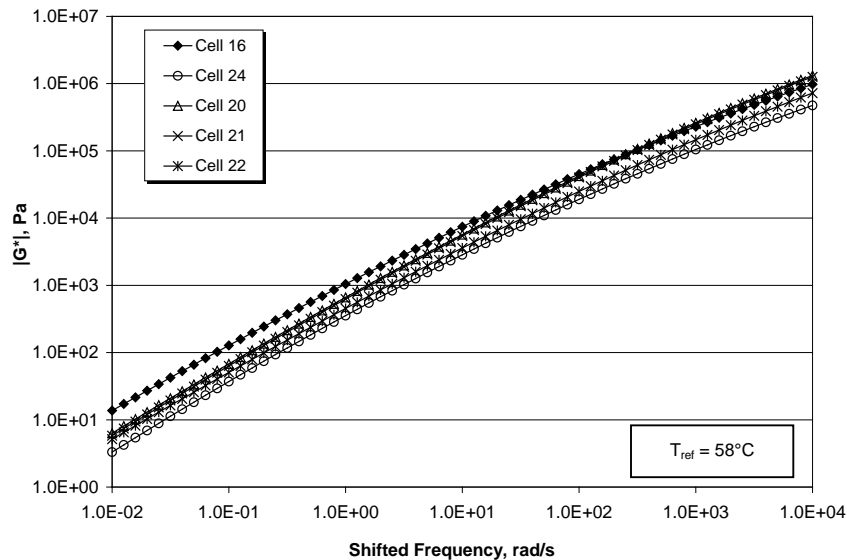


Figure 24 Extracted asphalt binder master curves.

It is interesting to note that the extracted binder from Cell 16 is stiffer than the other binders, even though this came from a mixture with PG 58-34 binder that used only 20% RAP with warm mix technology. The binder from the PG 64-34 WMA control section, Cell 24, was the softest across the entire temperature range. The other PG 58-34 binder was just slightly above this curve, due to the increase in RAP to 30%. The binders from the fractionated and regular RAP mixtures were indistinguishable, and they became the stiffest at the coldest temperature (depicted as high frequencies to the right of the graph).

Hirsch Model

The Hirsch model was first developed by T. J. Hirsch in the early 1960s and then refined in recent years by Christensen, Pellinen, and Bonaquist (13, 14, 15). The model estimates the modulus of asphalt concrete mixtures, a composite material, from binder stiffness data and volumetric properties.

Equation 3 presents the Hirsch model, which was the basis for this research.

$$|E^*|_{mix} = P_c \left[4,200,000(1 - VMA/100) + 3 |G^*|_{binder} \left(\frac{VFA \times VMA}{10,000} \right) \right] \\ + (1 - P_c) \left[\frac{1 - VMA/100}{4,200,000} + \frac{VMA}{3VFA |G^*|_{binder}} \right]^{-1}$$

Equation 3

where:

$$P_c = \frac{\left(20 + \frac{VFA \times 3 |G^*|_{binder}}{VMA} \right)^{0.58}}{650 + \left(\frac{VFA \times 3 |G^*|_{binder}}{VMA} \right)^{0.58}}$$

Equation 4

$|E^*|_{mix}$ = predicted dynamic modulus of the mixture, psi

VMA = voids in mineral aggregate, %

VFA = voids filled with asphalt, %

$|G^*|_{binder}$ = measured complex modulus of the binder, psi

In order to effectively use the Hirsch model on this data set, the binder and mixture data needed to be represented in consistent units. The first step in this process was to shift each binder master curve to 54.4°C, which was the temperature that the mixture master curves were constructed at. The binder shift factors (on a log scale) have a simple quadratic relationship with temperature, as shown in Figure 25 below. The binder master curves were then re-created at 54.4°C using the shift factors determined from the relationship demonstrated in Figure 25.

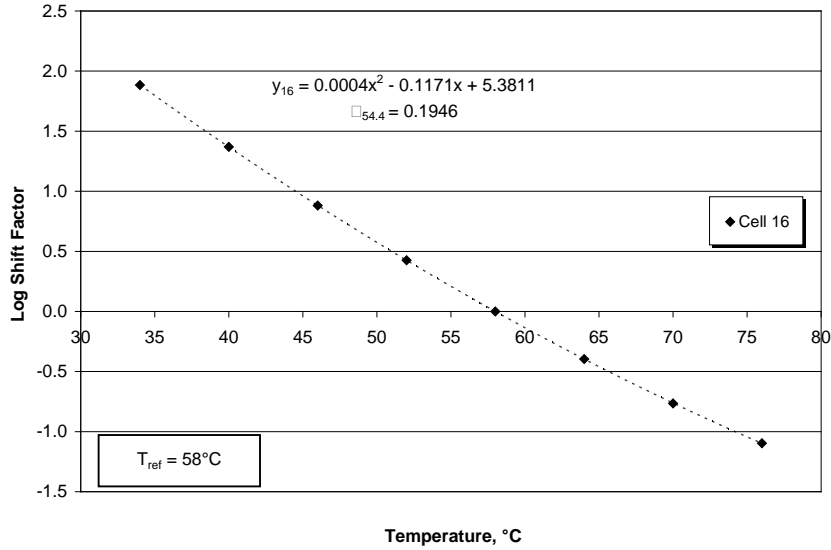


Figure 25 Example of shift factor vs. temperature curve for Cell 16.

The binder data was then converted from angular frequency in rad/s to Hz using Equation 5.

$$f = \frac{\omega}{2\pi}$$

Equation 5

Finally, both the binder and mixture modulus values were converted from GPa to psi to be consistent with the units in the Hirsch model. Using volumetric properties and binder stiffness data, the modulus of each asphalt mixture was then predicted using the Hirsch model as shown in Equation 3. The resulting master curves are shown in the following four plots.

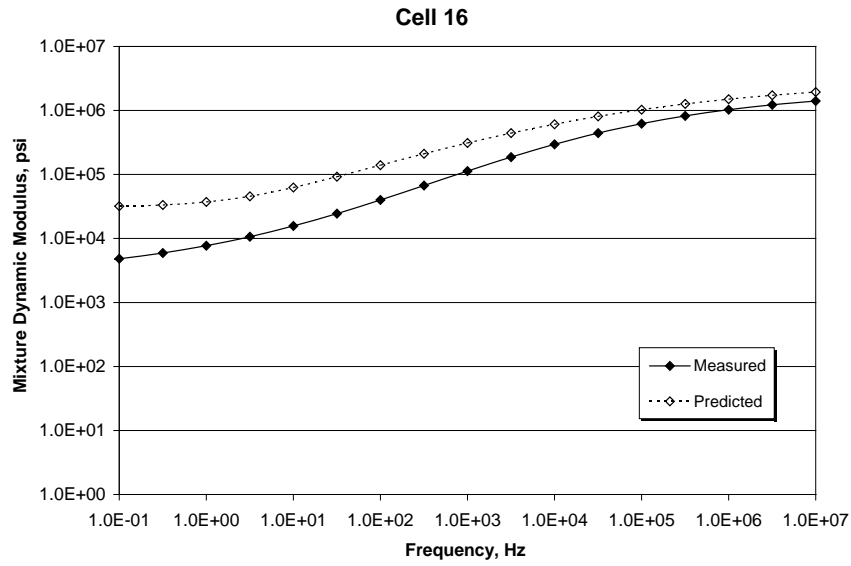


Figure 26 Hirsch model results for PG 58-34 WMA RAP 20%, Cell 16.

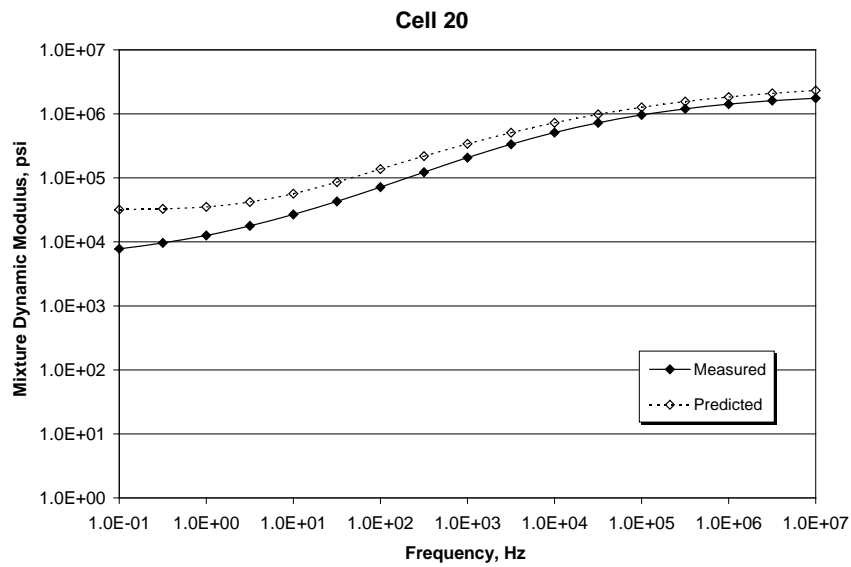


Figure 27 Hirsch model results for PG 28-28 HMA RAP 20%, Cell 20.

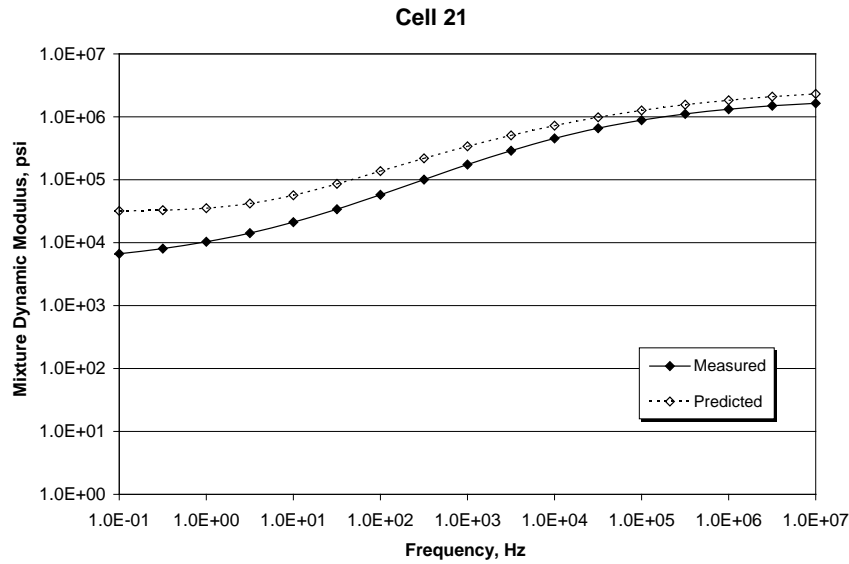


Figure 28 Hirsch model results for PG 58-28 HMA FRAP 30%, Cell 21.

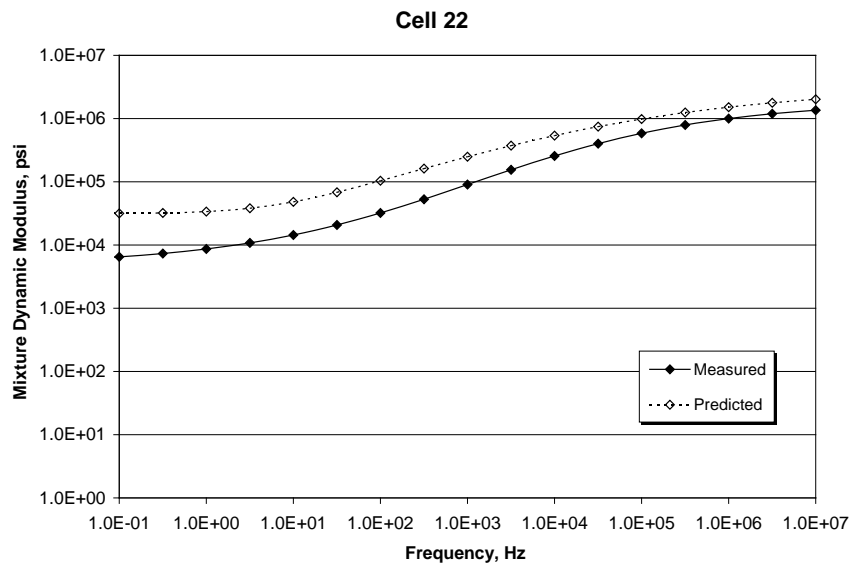


Figure 29 Hirsch model results for PG 58-34 HMA FRAP 30%, Cell 22.

Discussion

As has been discussed in reference (15) and elsewhere in the literature, the plots shown above can be a good qualitative means of determining whether or not the binder from the RAP fully blends with the virgin binder in the asphalt mixture. If the curve of predicted mix stiffness directly overlays the curve of measured stiffness, then good mixing has been achieved. If the predicted values fall above the measured values, then adequate blending did not occur. The predicted curve represents the fully blended condition, where the RAP and virgin binders are mixed during the extraction and recovery process. If the measured mixture curve is significantly

softer than the predicted curve, the indication is that the RAP is acting largely like “black rock” and the mix behavior is tied primarily to the virgin binder properties.

The data in this project shows that none of the mixtures achieved adequate blending between the RAP and virgin binders. Each of the predicted values is stiffer than those measured in the laboratory. In each case the diversion between predicted and measured curves can be seen most readily at intermediate and high temperatures (toward the middle and left of the graphs). At colder temperatures the curve line up more closely, perhaps a remnant of the fact that even old, severely aged RAP does not seem to diverge from its original low temperature PG grade nearly as much as its high temperature grade and therefore more closely resembles the behavior of the virgin binder.

The two mixtures with PG 58-28 binder and 30% RAP (Cells 20 and 21) show the most amount of blending, as the measured and predicted curves most closely match. The mixture from Cell 20 is the stiffest, and it appears to have the highest amount of blending between RAP and virgin binders. Fractionating the RAP, as in Cell 21, actually provided for less blending than when using RAP from a single stockpile, which is contrary to expectations. The researchers and many practitioners around the country have postulated that fractionating RAP will provide for better blending, and therefore a better product, at the hot mix plant.

The mixtures using PG 58-34 binders indicated a lesser amount of blending than those discussed above. Cell 22 had 30% fractionated RAP, but the measured and predicted curves were farther apart than those for Cell 21, an identical mixture with PG 58-28 binder. It is possible that the polymer modified binder in Cell 22 requires a higher mixing temperature simply to coat the aggregates, and if the proper temperature was not achieved at the plant it could at least partially account for the lesser degree of blending. The warm mix asphalt included only 20% RAP, but the predicted and measured curves were even farther apart. Apparently the lower production temperatures for warm mix (approximately 50 °F lower than hot mix) were not enough to activate the binder from the RAP and cause it to mix with the virgin binder.

The asphalt mixtures from this project were produced by a local contractor at a parallel flow drum plant. The RAP was added via a collar partway down the drum. In the case of the fractionated RAP mixes, the two different sizes were added from separate bins but added at the same time through the collar. Perhaps the plant type was such that the RAP did not have enough dwell time in the drum to sufficiently heat up and blend with the virgin components of the mixture. The haul time from the plant to the jobsite was approximately 20 minutes. While some additional blending between the RAP and virgin binders may occur simply by co-mingling for a time at elevated temperatures, it is possible that the mix was not stored long enough for this to occur.

Chapter 5: Conclusions and Observations

Summary and Recommendations

A number of laboratory tests were performed on mixtures from MnROAD Phase II that contained various percentages of RAP. The objective was to quantify differences between unblended component materials and between mixtures, with future field performance in mind. Mixtures were also evaluated to determine the amount of blending that occurred between the RAP and virgin binders. Dynamic modulus testing was performed on asphalt mixtures, while complex modulus testing was performed on extracted binders. The binder data was then used in the Hirsch model to predict the stiffness of the mixes. The major results of the testing and evaluation were:

- Extracted binder grades met or exceeded design values (Table 3, Table 4).
- Fracture energy from SCB data was useful in categorizing expected mixture performance in terms of recycle percentage (Table 10).
- The Hirsch model was an effective tool for assessing the amount of blending that occurred between RAP and virgin binders.
- The process of fractionating the RAP into two different sizes actually resulted in less blending than the mixture that incorporated the RAP as a single pile, contrary to what was expected.
- The mixtures using PG 58-28 binders indicated better blending than those with PG 58-34 binders. It is possible that the mixtures using polymer modified (PG 58-34) binders were not sufficiently heated at the plant to activate the binder in the RAP enough to blend with the virgin binder.
- The warm mix asphalt mixture showed the least amount of RAP and virgin binder blending of any of the mixtures at MnROAD. The combination of polymer modified binder and lower production temperatures due to the warm mix technology did not provide for adequate blending.
- Despite the concerns raised in this research, early pavement performance at MnROAD has shown that all five of these mixtures performed very well after four years in service. If durability of the mixtures is to be questioned, we would expect to see some pavement failures within a relatively short time frame.
- The authors recommend investigating other mixtures from Minnesota in a similar fashion to determine if the lack of blending in the mixtures studied was an isolated incident or if this is a more widespread problem. If it is found that many other mixtures around the state also suffer from a lack of virgin and RAP binder blending, the question then arises as to the long term performance of these pavements in the field.

Conclusions

While the points above addressed the lack of blending between RAP and virgin binders, what effect may this have on long term pavement performance? Conventional wisdom would argue that these asphalt mixtures would experience reduced durability and greater propensity for raveling, moisture damage, low temperature cracking, and fatigue cracking.

On the other hand, the Minnesota Department of Transportation (MnDOT) has been constructing asphalt pavements with RAP for over 30 years with great success. MnDOT's position is that pavements containing RAP perform as well as or better than those containing only virgin materials. As long as best practices have been followed regarding the handling and use of RAP, the result should be successful construction of sound, durable pavements.

Once the final field monitoring phase is completed, the materials included in this study will be compared for field versus laboratory performance. The results will be presented in the final report. The test sections will continue to be monitored over a five year period via a combination of laboratory and field testing. Distress surveys, falling weight deflectometer (FWD) testing, dynamic load testing, and other performance measures will be collected on a regular basis.

References

1. Proposal for State Project 8680-157 (T.H. 94 = 392), Minnesota Department of Transportation, 2007.
2. A. Johnson, T. Clyne, and B. Worel, “2008 MnROAD Phase II Construction Report”. Minnesota Department of Transportation, St. Paul, Minnesota, 2009.
3. E. Johnson and R. Olson, “LRRB Investigation 864 Task 1 Summary Report: Develop Literature Review and Agency Survey”. Mn/DOT Office of Materials, Maplewood, Minnesota, 2008.
4. E. Johnson, “LRRB Investigation 864 Task 2 Summary Report: Construction of Conventional and Fractionated RAP Test Cells at MnROAD”. Mn/DOT Office of Materials, Maplewood, Minnesota, 2011.
5. M. Watson and E. Johnson, “LRRB Investigation 864 Task 3 and 5 Summary Report: Annual Monitoring and Performance Report for Years 1 and 2”. Mn/DOT Office of Materials, Maplewood, Minnesota, 2011.
6. E. Johnson, “LRRB Investigation 864 Task 6 DRAFT Summary Report: Annual Monitoring and Performance Report for Year 3”. Mn/DOT Office of Materials, Maplewood, Minnesota, 2011.
7. M. Marasteanu, et al., “Investigation of Low Temperature Cracking in Asphalt Pavements”. Minnesota Department of Transportation, 2007.
8. Federal Highway Administration, “Asphalt Pavement Technology, Bituminous Mixtures Laboratory (BML) Equipment: SUPERPAVE Indirect Tensile Test”. www.fhwa.dot.gov/pavement/asphalt/labs/mixtures/idt.cfm. Accessed 2/7/2012.
9. M. Marasteanu, K.H. Moon, and M. Turos, “Asphalt Mixture and Binder Fracture Testing for 2008 MnROAD Construction”, Minnesota Department of Transportation, 2009. www.mrr.dot.state.mn.us/research/pdf/200942.pdf accessed May 15, 2012.
10. American Association of State Highway and Transportation Officials, “Standard Method of Test for Quantitative Extraction and Recovery of Asphalt Binder from Asphalt Mixtures”. AASHTO Designation T319, 2003.
11. ARA, Inc., ERES Consultants Division, *Guide for Mechanistic-Empirical Design of New and Rehabilitated Pavement Structures*, Final Report to the National Cooperative Highway Research Program, NCHRP, Washington, D.C., March 2004.
12. M. Marasteanu and D. Anderson, “Improved Model for Bitumen Rheological Characterization”. Eurobitume Workshop on Performance Related Properties for Bituminous Binders, Luxembourg, May 1999, paper no. 133.
13. H. Paul, “Evaluation of Recycled Projects for Performance”. Louisiana Transportation Research Center, Baton Rouge, Louisiana, 1995.
14. R. Bonaquist and D. Christensen, “Practical Procedure for Developing Dynamic Modulus Master Curves for Pavement Structural Design”. *Transportation Research Record No. 1929*, Transportation Research Board, Washington, D.C., 2005, pp. 208-217.
15. R. Bonaquist, “Can I Run More RAP?” *Hot Mix Asphalt Technology Magazine*, September/October 2007, pp. 11-13.